

# First Detection of a Pulsar above 100 GeV

**A. Nepomuk Otte (on behalf of the VERITAS Collaboration)**

Santa Cruz Institute for Particle Physics (SCIPP), Physics Department University of California Santa Cruz, 1156 High Street, Santa Cruz, CA 95064, USA

E-mail: nepomuk.otte@gmail.com

**Abstract.** We present the detection of pulsed gamma-ray emission from the Crab pulsar above 100 GeV with the VERITAS array of atmospheric Cherenkov telescopes [1]. Gamma-ray emission at these energies was not expected in pulsar models. The detection of pulsed emission above 100 GeV and the absence of an exponential cutoff makes it unlikely that curvature radiation is the primary production mechanism of gamma rays at these energies.

## 1. Introduction

One of the most powerful pulsars in gamma rays is the Crab pulsar [2, 3], PSR J0534+220, which is the remnant of a historical supernova that was observed in 1054 A.D. It is located at a distance of 6500 light years, has a rotation period of  $\approx 33$  ms, a spin-down power of  $4.6 \times 10^{38}$  erg  $s^{-1}$  and a surface magnetic field of  $3.78 \times 10^{12}$  G [4].

Within the corotating magnetosphere, charged particles are accelerated to relativistic energies and emit non-thermal radiation from radio waves through gamma rays. In general, gamma-ray pulsars exhibit a break in the spectrum between a few hundred MeV and a few GeV. Mapping the cut-off can help to constrain the geometry of the acceleration region, the gamma-ray radiation mechanisms and the attenuation of gamma-rays.

Although past measurements of the Crab pulsar spectrum are consistent with a power law with exponential cut-off, flux measurements above 10 GeV are systematically above the best-fit model, suggesting that the spectrum is indeed harder than a power law with exponential cut-off [3, 5]. However, the statistical uncertainty of the previous data was insufficient to allow a definite conclusion about the spectral shape. In this paper we summarise the recent detection of the Crab pulsar above 100 GeV with VERITAS.

## 2. Observation and analysis

VERITAS, the Very Energetic Radiation Imaging Telescope Array System, is an array of four 12 m diameter imaging atmospheric Cherenkov telescopes located in southern Arizona, USA [6]. After evidence for pulsed emission was seen in 45 hours of data from the Crab pulsar that were recorded between 2007 and 2010, a deep 62-hour observation was carried out on the Crab pulsar between September 2010 and March 2011. The observations were made in wobble mode with an 0.5 degree offset. After eliminating data taken under variable or poor sky conditions or affected by technical problems, the total analysed data set comprises 107 hours of observations (97 hours dead-time corrected) carried out with all four telescopes. The data were taken with the standard VERITAS trigger setting, and analysed with the standard VERITAS analysis tools. Details about the analysis can be found in [1].

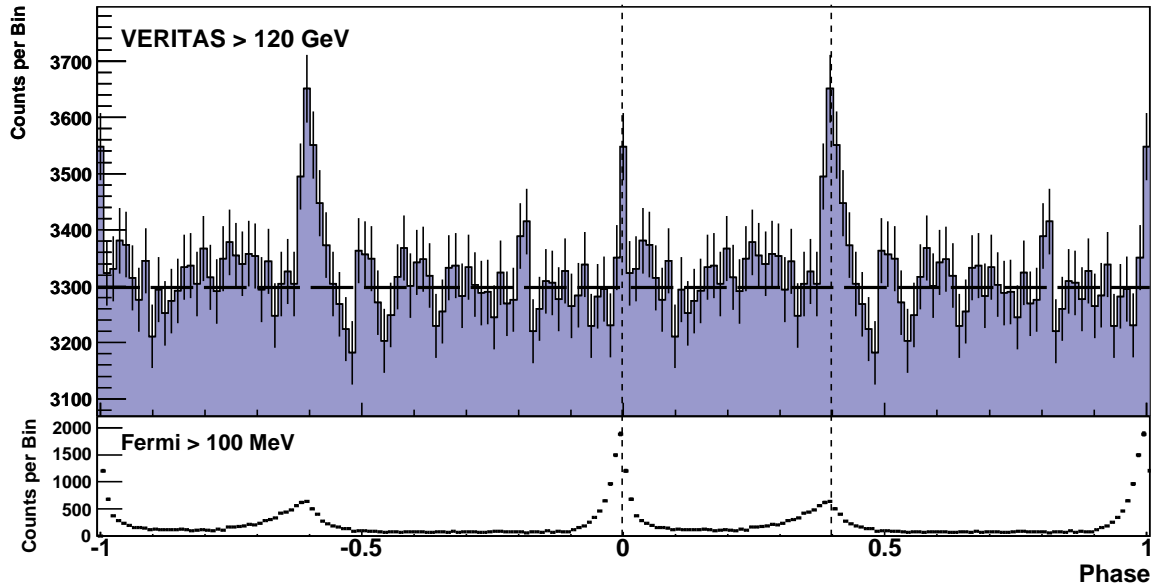


**Figure 1.** VERITAS pulse profile of the Crab pulsar at  $> 120$  GeV. The shaded histogram show the VERITAS data. The pulse profile is shown twice for clarity. The dashed horizontal line shows the background level estimated from data in the phase region between 0.43 and 0.94. The data above 100 MeV from the Fermi-LAT [3] are shown beneath the VERITAS profile. The vertical dashed lines in the panels mark the best-fit peak positions of P1 and P2 in the VERITAS data.

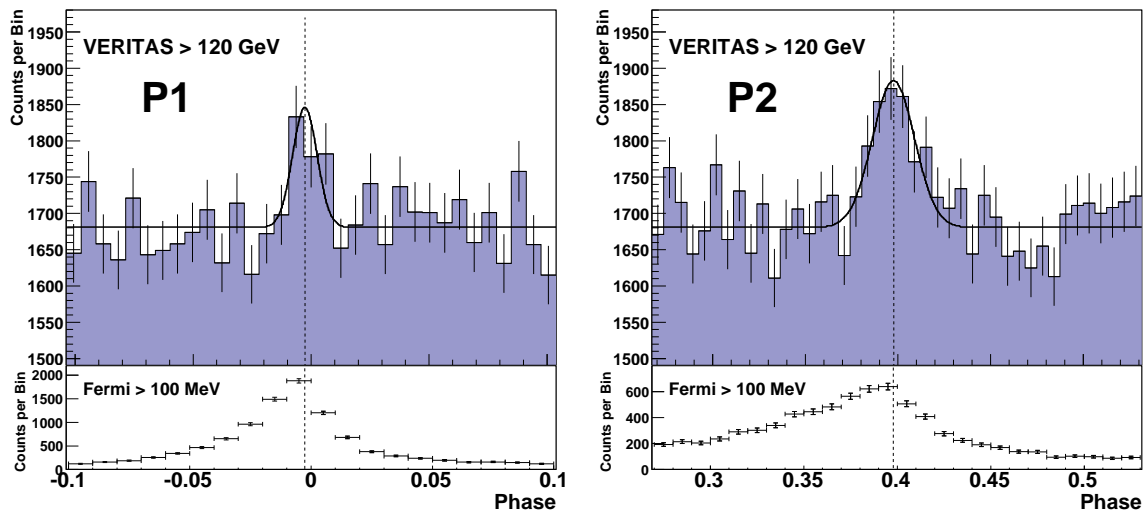
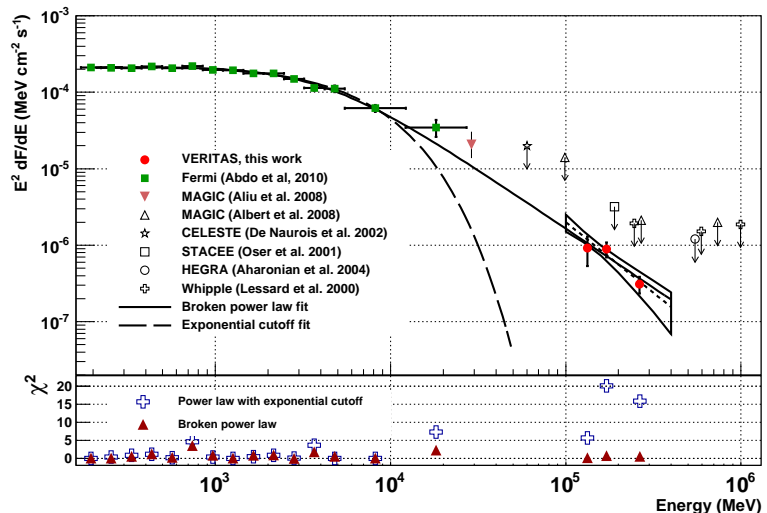


**Figure 2.** Enlarged view of the main pulse or **Figure 3.** Enlarged view of the interpulse or P1 of the Crab pulsar pulse profile. See text. P2 of the Crab pulsar pulse profile. See text.

**Figure 4.** Spectral energy distribution (SED) of the Crab pulsar in gamma rays. The bow tie and the enclosed dotted line give the statistical uncertainties and the best-fit power-law spectrum for the VERITAS data using a forward-folding method. The result of a fit of the VERITAS and Fermi-LAT data with a broken power law is given by the solid line and the result of a fit with a power-law spectrum multiplied with an exponential cut-off is given by the dashed line. Below the SED we plot  $\chi^2$  values to visualise the deviations of the best-fit parametrisation from the Fermi-LAT and VERITAS flux measurements.



### 3. Results

#### 3.1. Pulse Profile

The phase-folded event distribution, hereafter pulse profile, of the selected VERITAS events is shown in Figure 1. The most significant structures are two pulses with peak amplitudes at phase 0.0 and phase 0.4. These coincide with the locations of the main pulse and interpulse, hereafter P1 and P2, which are the two main features in the pulse profile of the Crab pulsar throughout the electromagnetic spectrum. In order to assess the significance of the pulsed emission, we use the H-Test [7]. The test result is 50, which translates into a statistical significance of 6.0 standard deviations that pulsed emission is present in the data.

The pulse profile has been characterised by an unbinned maximum-likelihood fit; see the solid black line in Figures 2 and 3. In the fit, the pulses are modeled with Gaussian functions, and the background is determined from the events that fall between phases 0.5 and 0.9 in the pulse profile (referred to as the off-pulse region).

The positions of P1 and P2 in the VERITAS data are thus determined to lie at the phase values  $-0.0026 \pm 0.0028$  and  $0.3978 \pm 0.0020$ , respectively, and are shown by the vertical lines Figure 1. The full widths at half maximum (FWHM) of the fitted pulses are  $0.0122 \pm 0.0035$  and  $0.0267 \pm 0.0052$ , respectively. The pulses are narrower than those measured by Fermi-LAT at 100 MeV by a factor of two to three. The energy-dependent narrowing of the pulses is a strong probe of the nature of the magnetospheric particle acceleration region and can be used to shed some light on its geometry, electric field, and gamma-ray emission properties.

#### 3.2. Spectrum

The gamma-ray spectrum above 100 GeV was measured by combining the signal regions around P1 (phase -0.013 to 0.009) and P2 (phase 0.375 to 0.421). This can be considered a good approximation of the phase-averaged spectrum. However, the existence of a flux component that originates in the magnetosphere and is uniformly distributed in phase cannot be excluded and would be indistinguishable from the gamma-ray flux from the nebula. Figure 4 shows the VERITAS phase-averaged spectrum together with measurements made with Fermi-LAT and MAGIC. In the energy range between 100 GeV and 400 GeV measured by VERITAS,

the energy spectrum is well described by a power law  $dN/dE = A \times (E/150 \text{ GeV})^\alpha$ , with  $A = (4.2 \pm 0.6_{\text{stat}} + 2.4_{\text{syst}} - 1.4_{\text{syst}}) \times 10^{-11} \text{ TeV}^{-1} \text{ cm}^{-2} \text{ s}^{-1}$  and  $\alpha = -3.8 \pm 0.5_{\text{stat}} \pm 0.2_{\text{syst}}$ . The detection of pulsed gamma-ray emission between 200 GeV and 400 GeV, the highest energy flux point, is only possible if the emission region is at least 10 stellar radii from the star's surface [8].

Combining the VERITAS data with the Fermi-LAT data we can place a stringent constraint on the shape of the spectral turnover. The previously favoured spectral shape of the Crab pulsar above 1 GeV was an exponential cut-off  $dN/dE = A \times (E/E_0)^\alpha \exp(-E/E_C)$ , which is a good parametrisation of the Fermi-LAT [3] and MAGIC [5] data. We note that the Fermi-LAT and MAGIC data can be equally well parametrised by a broken power law but those data are not sufficient to distinguish significantly between a broken power law and an exponential cut-off. The VERITAS data, on the other hand, clearly favour a broken power law as a parametrisation of the spectral shape. The fit of the VERITAS and Fermi-LAT data with a broken power law of the form  $A \times (E/E_0)^\alpha / [1 + (E/E_0)^{\alpha-\beta}]$  results in a  $\chi^2$  value of 13.5 for 15 degrees of freedom with the fit parameters  $A = (1.45 \pm 0.15_{\text{stat}}) \times 10^{-5} \text{ TeV}^{-1} \text{ cm}^{-2} \text{ s}^{-1}$ ,  $E_0 = 4.0 \pm 0.5_{\text{stat}} \text{ GeV}$ ,  $\alpha = -1.96 \pm 0.02_{\text{stat}}$  and  $\beta = -3.52 \pm 0.04_{\text{stat}}$  (see solid black line in Figure 2). A corresponding fit with a power law and an exponential cut-off yields a  $\chi^2$  value of 66.8 for 16 degrees of freedom. The fit probability of  $3.6 \times 10^{-8}$  derived from the  $\chi^2$  value excludes the exponential cut-off as a viable parametrisation of the Crab pulsar spectrum. The conclusions do not change if systematic uncertainties in the energy scale of both experiments are taken into account.

#### 4. Discussion

The detection of pulsed gamma-ray emission above 100 GeV provides strong constraints on the gamma-ray radiation mechanisms and the location of the acceleration regions. For example, the shape of the spectrum above the break cannot be attributed to curvature radiation because that would require an exponentially shaped cut-off. In addition, assuming a balance between acceleration gains and radiative losses by curvature radiation, the break in the gamma-ray spectrum is expected to be at  $E_{br} = 24 \text{ GeV } \eta^{3/4} \sqrt{\xi}$ , where  $\eta$  is the acceleration efficiency ( $\eta < 1$ ) and  $\xi$  is the radius of curvature in units of the light-cylinder radius [9]. Though  $\xi$  can be larger than one, only with an extremely large radius of curvature would it be possible to produce gamma-ray emission above 100 GeV with curvature radiation. It is, therefore, unlikely that curvature radiation is the dominant production mechanism of the observed gamma-ray emission above 100 GeV. Two possible interpretations are that either the entire gamma-ray production is dominated by one emission mechanism different from curvature radiation or that a second mechanism becomes dominant above the spectral break energy.

#### Acknowledgments

This research is supported by grants from the U.S. Department of Energy Office of Science, the U.S. National Science Foundation and the Smithsonian Institution, by NSERC in Canada, by Science Foundation Ireland (SFI 10/RFP/AST2748) and by STFC in the U.K. We acknowledge the excellent work of the technical support staff at the Fred Lawrence Whipple Observatory and at the collaborating institutions in the construction and operation of the instrument. A. N. Otte was in part supported by a Feodor Lynen fellowship from the Alexander von Humboldt Foundation.

#### References

- [1] E. Aliu et al. (VERITAS Collaboration), *Science*, 2011, 734 Vol. 334 no. 6052 pp. 69-72 DOI: 10.1126/science.1208192
- [2] J. M. Fierro et al., *ApJ*, 1998, **494**, 734

- [3] A. Abdo et al., *ApJ*, 2010, **708**, 1254
- [4] R. N. Manchester et al., *AJ*, 2005, **129**, 1993 <http://www.atnf.csiro.au/people/pulsar/psrcat/>
- [5] E. Aliu et al., *Science*, 2008, **322**, 1221
- [6] J. Holder et al., *Astroparticle Physics*, 2006, **25**, 391
- [7] O. C. de Jager, *ApJ*, 1994, **436**, 239
- [8] M. G. Baring, *Adv. Space Res.*, 2004, **33**, 552
- [9] Lyutikov, M., Otte, N., & McCann, A. 2011, arXiv:1108.3824